Full Dynamic Range Proteome Analysis of *S. cerevisiae* by Targeted Proteomics

Paola Picotti,[1] Bernd Bodenmiller,[1] Lukas N. Mueller,[1] Bruno Domon,[1] and Ruedi Aebersold[1,2,3,4,*]
[1]Institute of Molecular Systems Biology, ETH Zurich, Zurich CH 8093, Switzerland
[2]Competence Center for Systems Physiology and Metabolic Diseases, Zurich CH 8093, Switzerland
[3]Institute for Systems Biology, Seattle, WA 98103, USA
[4]Faculty of Science, University of Zurich, Zurich CH 8057, Switzerland
*Correspondence: aebersold@imsb.biol.ethz.ch

SUMMARY

The rise of systems biology implied a growing demand for highly sensitive techniques for the fast and consistent detection and quantification of target sets of proteins across multiple samples. This is only partly achieved by classical mass spectrometry or affinity-based methods. We applied a targeted proteomics approach based on selected reaction monitoring (SRM) to detect and quantify proteins expressed to a concentration below 50 copies/cell in total *S. cerevisiae* digests. The detection range can be extended to single-digit copies/cell and to proteins undetected by classical methods. We illustrate the power of the technique by the consistent and fast measurement of a network of proteins spanning the entire abundance range over a growth time course of *S. cerevisiae* transiting through a series of metabolic phases. We therefore demonstrate the potential of SRM-based proteomics to provide assays for the measurement of any set of proteins of interest in yeast at high-throughput and quantitative accuracy.

INTRODUCTION

The ability to reliably identify and accurately quantify any protein or set of proteins of interest in a proteome is an essential task in life science research. This has been attempted by two general experimental approaches. The first is based on the generation of affinity reagents exemplified by highly specific antibodies and the development of an array of methods to deploy them for detecting and quantifying specific proteins in complex samples. The second is mass spectrometry (MS)-based quantitative proteomics that attempts to identify and quantify all proteins contained in a sample.

Multiple versions of affinity reagent-based methods (e.g., the broadly used western blot or ELISA approaches) have been implemented. They differ in the type of affinity reagent and detection system used (Uhlen, 2008). The methods with the highest sensitivity have the potential to detect, in principle, low-abundance proteins, with zeptomole detection limits already demonstrated (Pawlak et al., 2002). However, the development of sets of reagents of suitable specificity and affinity to support the conclusive detection and quantification of target protein(s) remains challenging, expensive, and arduous, and coordinated efforts to develop validated affinity reagents are just getting underway (Taussig et al., 2007; Uhlen and Hober, 2009). The methods based on affinity reagents are therefore limited by slow assay development and, usually, also by the inability to significantly multiplex detection of proteins in the same sample.

Similarly to affinity-based methods, a wide range of MS-based proteomic methods have been developed. The most successful of these, in terms of number of proteins identified, use a shotgun strategy in which a subset of peptides present in a tryptic digest of a proteome is selected in an intensity-dependent manner for collision-induced dissociation by a tandem mass spectrometer (Aebersold and Mann, 2003). The resulting fragment ion (MS/MS) spectra are then assigned to sequences in a peptide database and the corresponding peptides and proteins are thus identified. This method provides accurate quantitative data if suitable stable isotope-labeled references are available and included in the analysis (Desiderio and Kai, 1983; Gerber et al., 2003). However, these methods are nontargeted, i.e., in each measurement they stochastically sample a fraction of the proteome that is usually biased toward the higher end of the abundance scale (Domon and Broder, 2004; Picotti et al., 2007). Each repeat analysis required for comparing a proteome at different states will sample only a subset of the proteins it contains and not necessarily the same subset in each repeat, thus precluding the generation of complete and consistent data sets (Wolf-Yadlin et al., 2007). More extensive, although still incomplete and stochastic, proteome coverage can be achieved in large proteome mapping experiments, whereby the proteome is extensively fractionated by multiple approaches and the content of each fraction is sequenced to saturation (Chen et al., 2006; de Godoy et al., 2006, 2008). Such studies carry a significant experimental and computational overhead and are therefore time/labor consuming and can be performed only in highly specialized laboratories. In addition, they mostly retain
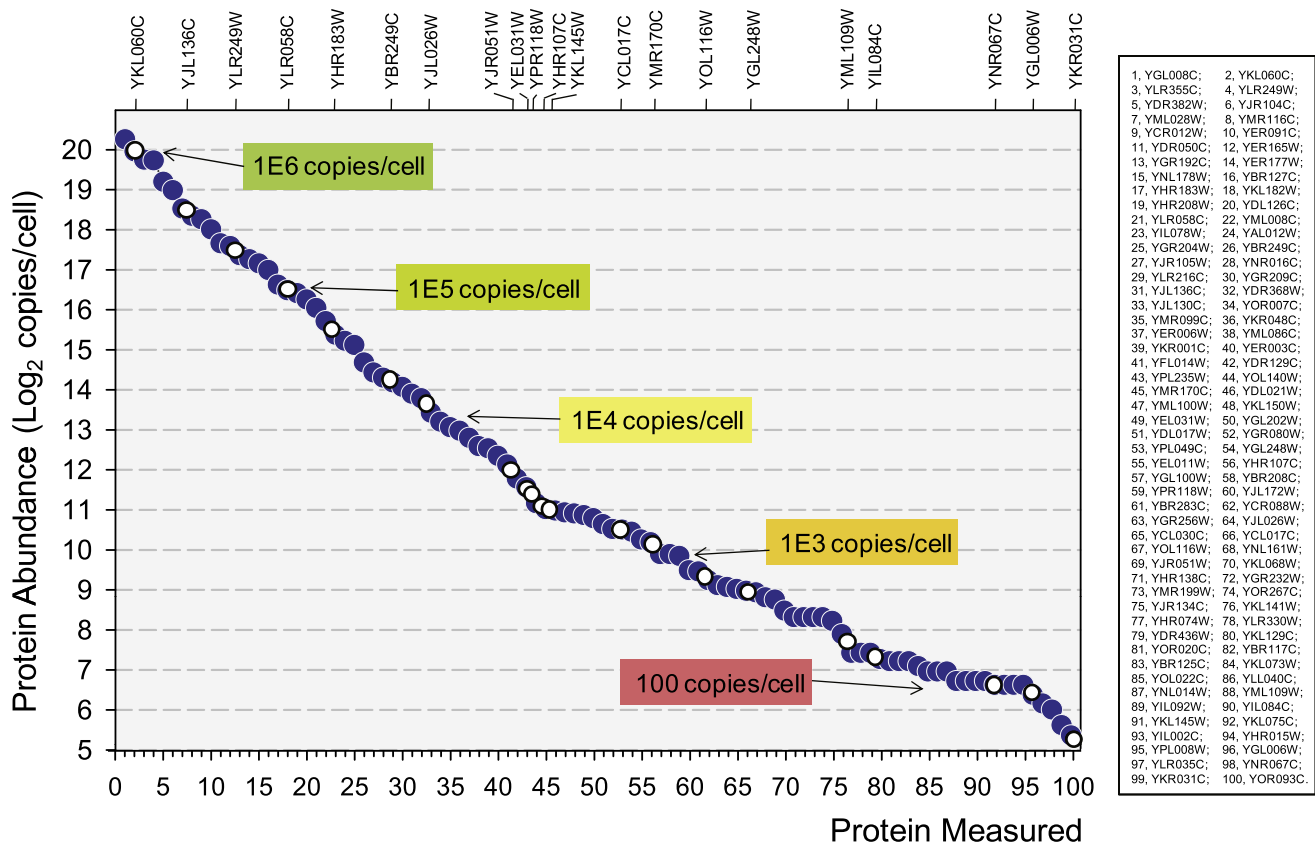
Figure 1. Cellular Concentrations of the Set of Measured Proteins
Protein abundances are derived from Ghaemmaghami et al. (2003). Proteins detected by SRM assays are sorted by abundance to show the even distribution across the whole range of concentration (blue circles). Proteins for which the absolute abundance was measured using isotopically-labeled standards are indicated on top of the graph (open circles).

the bias against low-abundance proteins, albeit to a reduced degree. This makes such approaches impractical in cases that require the consistent quantification of sets of proteins of all abundances across a variety of different samples and replicates.

To alleviate these limitations, we demonstrate in this study the potential of selected reaction monitoring (SRM)-based targeted MS (Anderson and Hunter, 2006; Lange et al., 2008) to provide specific assays for the detection and quantification of proteins over the whole range of cellular concentrations in *S. cerevisiae*. We deploy the approach to quantitatively monitor the dynamics of a protein network containing proteins spanning a broad range of abundances, across numerous samples and replicates, at high speed and quantitative accuracy.

RESULTS

Detection of Low-Abundance Proteins in a Total Yeast Cell Lysate by SRM

We challenged the dynamic range of SRM-based targeted proteomics by applying it to the detection and quantification of yeast proteins distributed across the whole range of cellular abundance, with the purpose of determining to what concentration (in copies/cell) yeast proteins can be detected in a tryptic digest

of a total cell lysate. We selected protein targets based on the list of absolute protein abundances generated by orthogonal methods (i.e., by quantitative western blotting against a tandem affinity purification tag engineered into *S. cerevisiae* genes [Ghaemmaghami et al., 2003]). We selected a set of 100 target proteins evenly distributed across all levels of cellular abundance, from 1.3E6 to 41 copies/cell (Figure 1) in *S. cerevisiae*. These proteins were grouped into the copy number classes indicated in Table 1 (groups 1–14). Each class minimally contained five proteins. The classes with proteins of lower abundance contained a higher number of proteins to increase the significance of low-copy number protein detection. For each protein, five proteotypic peptides (unique peptides preferentially detectable by MS [PTPs] [Brunner et al., 2007; Kuster et al., 2005]) were selected. PTPs were derived by screening a large yeast proteomic data repository, *PeptideAtlas* (>36,000 unique peptides observed in an array of shotgun proteomic experiments [Deutsch et al., 2008]) for the most frequently observed peptides for each target protein. For proteins for which fewer than five PTPs could be extracted from *PeptideAtlas*, additional peptides with favorable MS properties were derived by bioinformatic prediction using the tool *PeptideSieve* (Mallick et al., 2007). For each PTP an SRM assay consisting of three optimal and validated

Table 1. Summary of Proteins Detected and Quantified in Each Group of Cellular Abundance

Abundance Range (Copies/Cell)	Group	Proteins Measured	Protein Names[a]	Absolute Quantification[b]
524,288–1,255,722	1	5	YGL008C, YKL060C, YLR355C, YLR249W, YDR382W	YKL060C
262,144–524,288	2	5	YJR104C, YML028W, YMR116C, YCR012W, YER091C	YJL136C
131,072–262,144	3	5	YDR050C, YER165W, YGR192C, YER177W, YNL178W	YLR249W
65,536–131,072	4	5	YBR127C, YHR183W, YKL182W, YHR208W, YDL126C	
32,768–65,536	5	5	YLR058C, YML008C, YIL078W, YAL012W, YGR204W	YHR183W, YLR058C,
16,384–32,768	6	5	YBR249C, YJR105W, YNR016C, YLR216C, YGR209C	YBR249C
8,192–16,384	7	5	YJL136C, YDR368W, YJL130C, YOR007C, YMR099C	YJL026W
4,096–8,192	8	5	YKR048C, YER006W, YML086C, YKR001C, YER003C	
2,048–4,096	9	5	YFL014W, YDR129C, YPL235W, YOL140W, YMR170C	YEL031W, YHR107C, YPR118W, YJR051W
1,024–2,048	10	10	YDL021W, YML100W, YKL150W, YEL031W, YGL202W, YDL017W, YGR080W, YPL049C, YGL248W, YEL011W	YMR170C, YCL017C
512–1,024	11	10	YHR107C, YGL100W, YBR208C, YPR118W, YJL172W, YBR283C, YCR088W, YGR256W, YJL026W, YCL030C	YOL116W
256–512	12	10	YCL017C, YOL116W, YNL161W, YJR051W, YKL068W, YHR138C, YGR232W, YMR199W, YOR267C, YJR134C	YGL248W
128–256	13	10	YKL141W, YHR074W, YLR330W, YDR436W, YKL129C, YOR020C, YBR117C, YBR125C, YKL073W, YOL022C	YIL084C, YML109W
<128	14	15	YLL040C, YNL014W, YML109W, YIL092W, YIL084C, YKL145W, YKL075C, YIL002C, YHR015W,YPL008W, YGL006W, YKR031C, YLR035C, YNR067C, YOR093C	YGL006W, YNR067C, YKR031C
No expression detected[a]	15	15	YDR381W, YNL208W, YHR020W, YNL160W, YEL024W, YJL008C, YJL111W, YFL037W, YDR023W, YJR123W, YLR340W, YJR077C, YDR321W, YCL018W, YER055C	
Below QOD (<50 copies/cell)[a]	16	6	YBR006W, YCL043C, YDR150W, YOR120W, YJL167W, YBR006W	
Western blot band not quantifiable[a]	17	6	YHR029C, YNL055C, YJL080C, YDL140C, YIR006C, YGR284C	
Never observed in publicly accessible proteomics data sets[c]	18	10	YDL017W, YOL116W, YBR117C, YIL092W, YKL075C, YIL002C, YHR015W, YPL026C, YLR035C, YOR093C	

[a] Abundances and categorization according to Ghaemmaghami et al. (2003).
[b] Abundances are as derived from SRM measurements.
[c] As derived from the absence of the protein in *PeptideAtlas*.

precursor ion to fragment ion transitions was developed on a triple quadrupole mass spectrometer (see the Experimental Procedures). For low-abundance proteins, critical MS parameters were specifically optimized to maximize the sensitivity of the corresponding assay. For each protein the SRM assays associated with the two best responding PTPs were used in final measurements. The resulting assays were then applied to detect and/or quantify the target proteins in unfractionated trypsinized extracts of *S. cerevisiae* cells, grown under the conditions described by Ghaemmaghami et al. (2003). Data were acquired in time-scheduled SRM mode to maximize throughput and sensitivity (Stahl-Zeng et al., 2007). The results indicate that proteins spanning a range of literature abundance values from over a million down to 41 copies/cell could be unambiguously detected. Approximately 10% of the targeted proteins could not be detected. A list of these proteins and a rationale for the inability to detect them is presented in Table S1 (available online). Both the cellular abundances (1.3E6 to 41 copies/cell) of the set of proteins de-

tected in an unfractionated yeast digest and the associated SRM signal intensities covered a range of ~4.5 orders of magnitude. The linear correlation between the abundance of proteins and the SRM signal intensity of the respective most intense PTPs (log scale) is shown in Figure S3. These results demonstrate that SRM-based proteomics has the power to reliably detect proteins expressed in the whole range of documented cellular abundance, down to a concentration of <50 protein copies/cell in *S. cerevisiae* total cell digests without the need of sample fractionation or enrichment.

Absolute Quantification of Proteins in a Total Cell Lysate
To confirm that the abundance range of the detected proteins truly reflected the literature values described by Ghaemmaghami et al. (2003), we used stable isotope-labeled reference peptides to absolutely quantify 21 selected proteins distributed across all levels of cellular abundances (Table 2). In most cases the measured absolute protein abundances closely matched the

Table 2. Absolute Quantification of Proteins Spanning the Whole Range of Abundances Using Heavy Peptide Standards

Protein	Measured Abundance (Copies/Cell)[a]	Literature Value (Copies/Cell)[b]	Standard Deviation of Measured Abundance
YKL060C	996,503	1,018,216	51,818
YLR249W	189,235	870,578	30,864
YHR183W	48,926	101,441	7,354
YLR058C	98,940	67,559	15,860
YBR249C	19,459	26,272	5,083
YJL136C	370,314	15,300	41,142
YMR170C	1,114	2,072	217
YEL031W	3,125	1,873	472
YGL248W	501	1,404	68
YHR107C	2,317	1,169	144
YPR118W	2,631	922	477
YJL026W	13,871	538	1,144
YCL017C	1,508	504	229
YOL116W	614	491	154
YJR051W	3,912	432	911
YIL084C	162	105	31
YML109W	215	105	39
YKL145W	2,114	105	234
YGL006W	90	99	19
YNR067C	103	64	14
YKR031C	39	49	9

[a] Data are expressed as mean values.
[b] As derived from Ghaemmaghami et al. (2003).

Figure 2. Analysis of the SRM Signal Gain Obtained by Peptide Fractionation
Peptide fractionation was achieved by OGE of a total yeast digest in 24 wells, using 3–10 pI strips. For each peptide the signal gain compared to the unfractionated peptide mixture resulting from the highest SRM transition and the highest concentration fraction is reported using a logarithmic scale (left axis). Vertical bars show the mean signal gain in each fraction. The peptide pI associated to each fraction is also reported (right axis) as mean ± standard deviation, as derived from large-scale shotgun proteomic experiments in which more than 55,000 yeast peptides were identified across the 24 OGE fractions (data not shown).

published values. For 17 of these proteins the two measured abundance values deviated by less than a factor of three, with the closest values deviating by less than 10%. Four proteins deviated more than 5-fold from the published values. The protein with the lowest abundance was measured at ~40 copies/cell and the highest at over 1E6 copies/cell. These results confirm the quality of the reference list (Ghaemmaghami et al., 2003) and demonstrate that proteins expressed to a concentration of <50 copies/cell could be detected and quantified by SRM in total yeast lysates.

Increase of Sensitivity and Dynamic Range by a Simple Sample Fractionation Step

We next asked whether the addition of a single sample fractionation step would further increase the detection sensitivity of the method, due to reduction of sample complexity, to single-digit copy/cell numbers. We therefore fractionated peptides in a tryptic yeast digest by isoelectric focusing (Malmstrom et al., 2006) using an off-gel electrofocusing (OGE) system, with 24 fractions collected, spanning a 3–10 pI range. Peptides in each fraction were analyzed via scheduled SRM, using the previously validated SRM assays. Overall, 260 peptides were monitored across the 24 OGE fractions and for each peptide the fraction associated with the highest SRM signal and the corresponding signal intensity were derived. Figure 2 shows for every peptide the maximum

signal intensity gain achieved by OGE fractionation compared to the signal obtained for the same peptide in the unfractionated peptide mixture. Overall the average signal gain obtained by peptide fractionation was ~10-fold. The highest signal gain was realized in the fractions corresponding to low pI peptides (fractions 1–5, pI < 5), with a maximum in the first fraction (average ~25-fold increase and up to ~80-fold) (see the Supplemental Data for a discussion of the underlying reasons). The signal gain showed no correlation with the protein abundance or the retention time of the peptide (data not shown). These results show that pI-based enrichment of the targeted PTPs by OGE realized a maximal signal gain of more than 50-fold and an average gain of about 10-fold compared to the signal recorded from an unfractionated sample. This demonstrates that proteins expressed at a single-digit number of copies/cell can be detected by SRM coupled to a simple, fast, and predictable sample fractionation step.

Detection of Previously Undetected *S. cerevisiae* Proteins

Given the analytical depth achieved by the SRM-based approach we asked whether the method has the potential to detect proteins that have been undetectable by other techniques. We assembled a set of proteins (Table 1) that were not detected before, either by the affinity-based technique (Ghaemmaghami et al., 2003) (Table 1, groups 15–17) or by in-depth shotgun proteomics (Table 1, group 18), as determined by their absence in the largest publicly accessible proteomic database *PeptideAtlas*. To target proteins that had not been detected by the affinity-based method we followed the approach described

above. To target proteins never observed in proteomics experiments we used unpurified synthetic peptides to generate SRM assays for peptides from each of the targeted proteins. For each protein five PTPs likely to be observed by MS were predicted with *PeptideSieve* and synthesized on a microscale using the SPOT synthesis (Hilpert et al., 2007; Wenschuh et al., 2000). The peptides were used as a reference for deriving the final optimal coordinates of the SRM assays and for validating the assays. The assays developed were then applied to detect the proteins in a total yeast cell lysate by scheduled SRM. Overall, of the 45 targeted proteins 37 could be unambiguously detected in the unfractionated yeast digest (Table 1, and see also Table S1). The observed SRM signal intensities covered a range of approximately two orders of magnitude. The highest signals were related to proteins that did not express in a tagged format (Ghaemmaghami et al., 2003). The lowest signal intensities were from proteins not previously detected by proteomics techniques or from those below the detection/quantification limits in the reference method (Ghaemmaghami et al., 2003) (Table 1). These results demonstrate that SRM-based proteomics is capable of measuring proteins that have been undetectable by other methods and therefore of detecting and quantifying previously unknown segments of the yeast proteome. Cumulatively, these results demonstrate the potential of SRM-based proteomics to map out the whole MS-observable yeast proteome and provide assays for the detection/quantification of proteins expressed at a concentration above single-digit copies/cell in *S. cerevisiae*.

Application to a Biological Protein Network

In order to demonstrate the power of the technique when applied to the analysis of a biological system, we targeted a network of 45 proteins in the central carbon metabolism of *S. cerevisiae* (Figure 3A). This pathway is an ideal example to demonstrate the dynamic range of the technique since it contains proteins that range from extremely high concentrations (ALF/YKL060C, 1.0E6 copies/cell, third most abundant protein in *S. cerevisiae*, based on Ghaemmaghami et al. [2003]) to very low (ADH4/ YGL256W, <128 copies/cell) and also contains proteins whose abundance could not be measured by the tandem affinity purification tagging approach (e.g., LSC2/YGR244C) (Figures 3A and 3B) (Ghaemmaghami et al., 2003). For each protein in the set we developed SRM assays as described above and applied them to measure the proteins in an unfractionated yeast digest, using scheduled SRM (Figure 3C). The protein network composed of proteins at all abundance levels could be measured using a single 30 min chromatographic gradient, corresponding to <1 hr total MS analysis time. In most cases proteins could be measured via two peptides/protein, each peptide was monitored via three SRM transitions and each SRM-chromatographic peak contained at least eight data points, which ensured reliable quantification of the eluting peptide. The SRM assays used in this study are available in Tables S5 and S6 or via the MRMAtlas interface (http://www.mrmatlas.org) (Picotti et al., 2008).

We next applied the validated SRM transitions for the whole protein network described above to generate complete quantitative profiles for each protein over a time course of the dynamic growth of *S. cerevisiae*, covering a series of different growth phases and a metabolic shift. We sampled the cultures at ten time points in biological triplicate while they transited from exponential growth in a glucose-rich medium, through the diauxic shift and consequent fermentative growth on ethanol, to the entrance in the stationary phase (Figures 4A and 4B). The temporal boundaries of the growth phases were established by monitoring the cell density in the medium as a measure of the growth rate, the consumption of extracellular glucose, and the accumulation of ethanol in the medium (Figures 4A and 4B). The total 30 samples were subjected to scheduled SRM analysis and the resulting data were compiled to derive the quantitative profile, normalized to the first time point (6.5 hr), for each protein over the dynamic growth profile. Average values are shown out of the three biological replicates in Figure 4C. Proteins were grouped by unsupervised clustering on the basis of their expression profiles into three clusters. Cluster 1 (Figures 4C and 4D) predominantly contained enzymes in the glyoxylate cycle and enzymes responsible for the catalysis of the backward or shortcut reactions required to revert flux directions upon the shift (DeRisi et al., 1997). These proteins showed a marked induction (up to 380-fold, average cluster 210-fold) upon the diauxic shift and their levels remained constant or showed only slight reduction during the respiratory growth and at the entrance of the stationary phase. Cluster 2 (Figures 4C and 4E) mostly contained enzymes involved in the tricarboxylic acid (TCA) cycle that were coordinately induced upon the diauxic shift by up to 22-fold (cluster average induction 8-fold) and then showed a slow decrease in abundance during the slow respiratory growth and the beginning of the stationary phase. Cluster 3 (Figures 4C and 4F) predominantly contained glycolytic enzymes that did not show pronounced abundance changes throughout the whole series of different metabolic phases. The postdiauxic induction was statistically significant ($p < 0.05$ and fold change >2; see Table S4) for all proteins in clusters 1 and 2, except for pyk2 ($p = 0.063$). The coefficient of variation (CV%) of the measurements was on average ~15% and the data required in total <2 days of MS time. These data demonstrate the capacity of SRM-based proteomics to comprehensively and reproducibly measure sets of biologically related proteins spanning the whole range of abundances in a single MS run at high-throughput and quantitative accuracy.

We next correlated the protein profiles generated in this study with corresponding transcript profiles to detect potential posttranscriptional regulation during the metabolic shift. We compared the protein abundance profiles to a reference microarray data set for the diauxic shift in *S. cerevisiae* (DeRisi et al., 1997). The two data sets were acquired under closely similar experimental conditions and the time course profiles were realigned, normalized, and compared in the growth region associated to the shift (time points 1–6). We detected four general correlation patterns between protein and transcript abundance changes (Figure 5A). The first pattern (Figure 5A, region 1) showed cases where protein and mRNA abundances were both increasing. In the second pattern (Figure 5A, region 2) both types of molecules decreased abundances. The third pattern showed cases where protein abundance increased and mRNA abundance decreased and the fourth pattern showed cases where protein abundance decreased and mRNA abundance increased. Most of the measurements populated group 1 or 2, indicating that
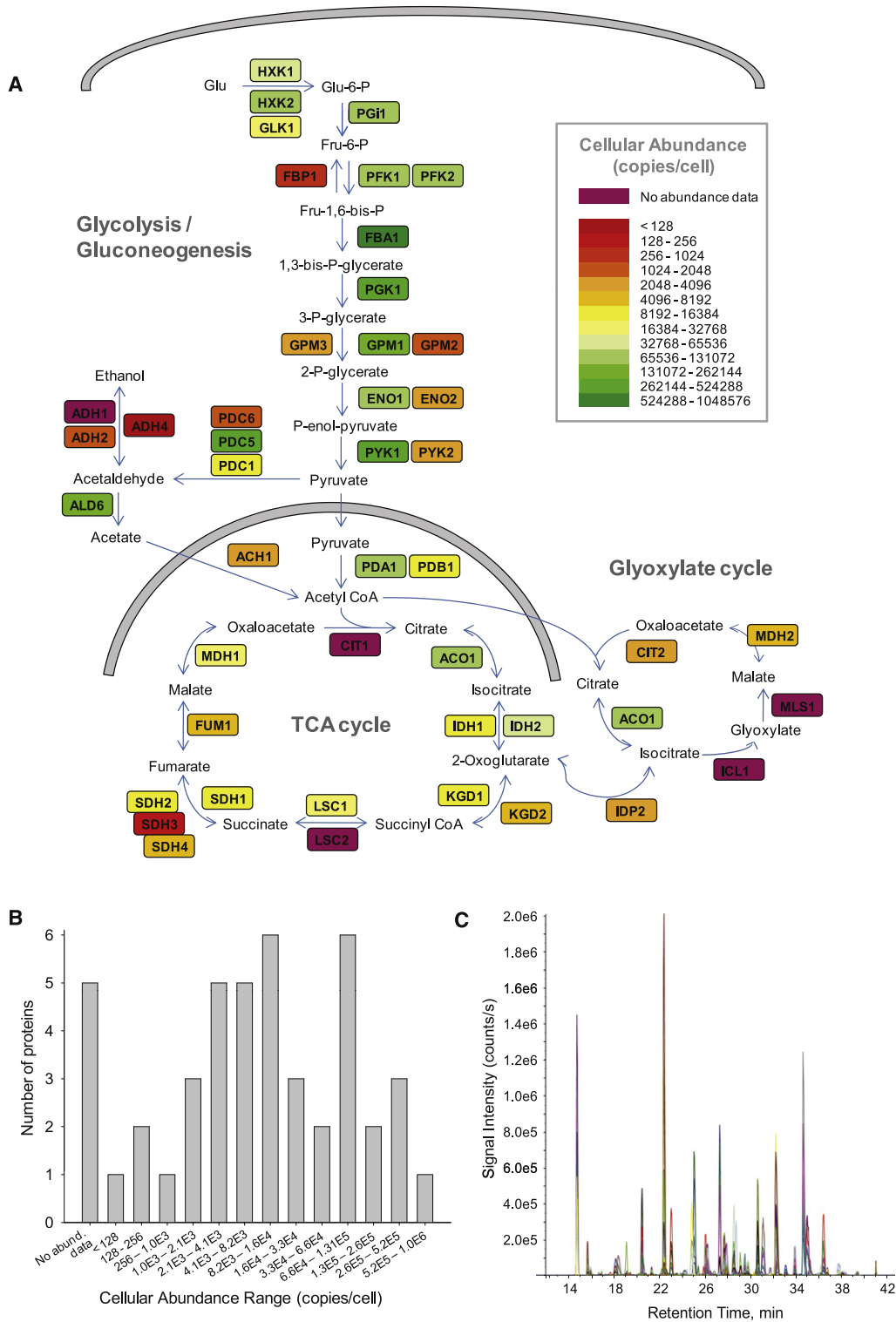
Figure 3. SRM Analysis of a Biological Protein Network

(A) Schematic representation of a core protein network (glycolysis/gluconeogenesis/TCA cycle/glyoxylate cycle) in the central carbon metabolism of *S. cerevisiae.* Proteins are colored according to their absolute abundances as measured by Ghaemmaghami et al. (2003).

(B) Distribution of the cellular abundances of the 45 proteins composing the network. For each protein, an SRM assay was developed and applied to detect the protein in an unfractionated yeast digest, using scheduled SRM, in a single MS analysis.

(C) LC-SRM chromatogram comprising the whole set of SRM assays for proteins in the network. Each peak represents an SRM assay that detects a tryptic peptide of one of the target proteins in the total yeast digest.
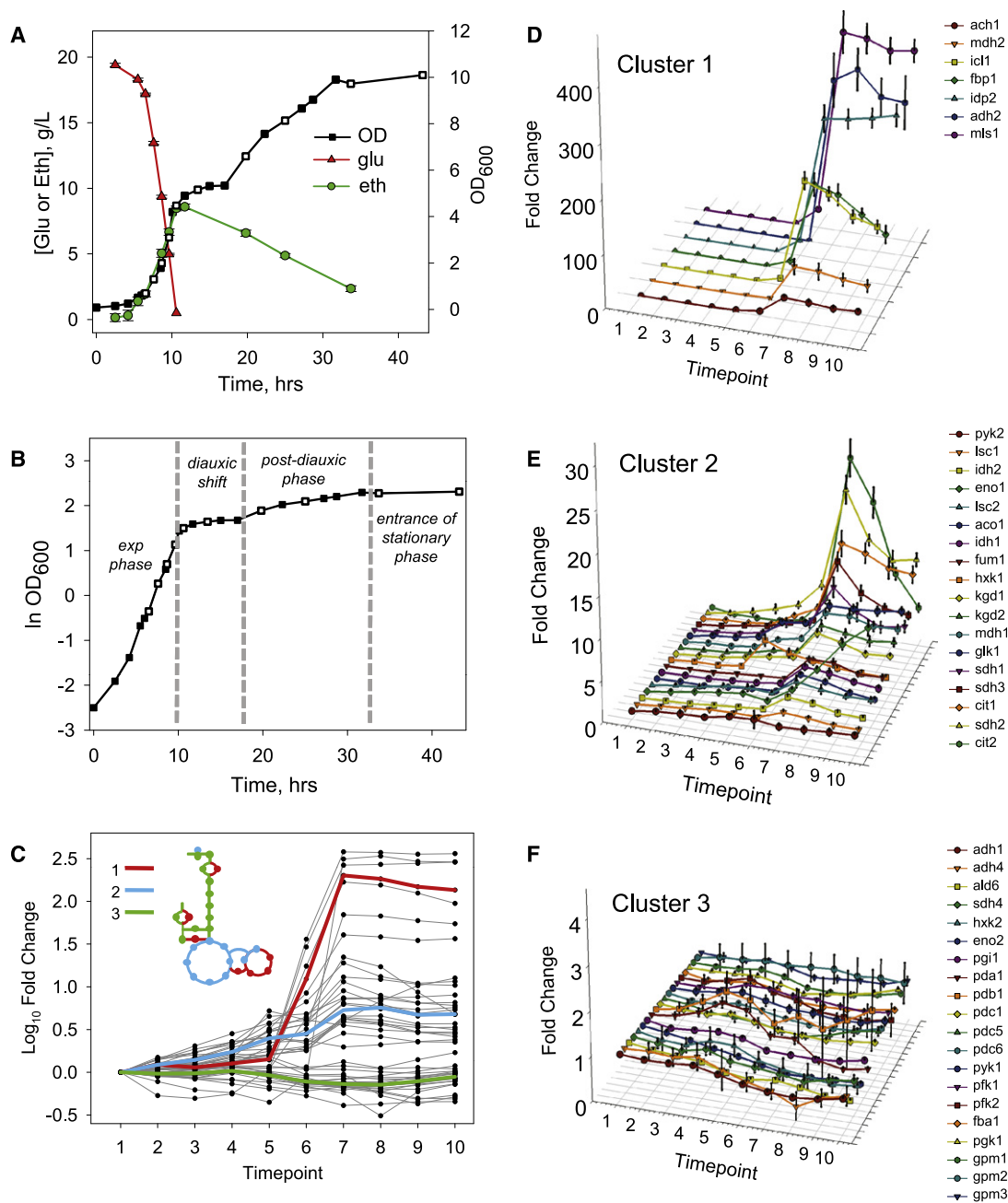
Figure 4. Time Course Analysis of the Central Carbon Metabolism Protein Network along the Dynamic Growth Profile of *S. cerevisiae* in a Glucose-Rich Medium

(A) Growth profile, as followed by monitoring the optical density at 600 nm (OD_{600}) of the culture, and the extracellular glucose and ethanol concentrations.

(B) Different growth phases occurring during *S. cerevisiae* growth in a glucose-rich medium. The growth profile is plotted using a log_{10} scale to better highlight the transition regions. Protein sampling time points are represented as open squares in (A) and (B) (T1, 6.5 hr; T2, 7.6 hr; T3, 8.7 hr; T4, 9.6 hr; T5, 10.6 hr; T6, 11.7 hr; T7, 19.8 hr; T8, 25.0 hr; T9, 33.7 hr; T10, 43.2 hr).

(C) Measured abundance profiles for all the proteins in the protein network under study, along the growth curve. Mean abundance changes out of three biological replicates with respect to time point 1 (6.5 hr) are plotted using a log_{10} scale. Profiles of the three clusters deriving from the clustering analysis are shown in color. A schematic representation of the system under study highlights proteins belonging to each cluster in the corresponding color.

(D–F) Abundance profiles for each protein belonging to cluster 1 (D), 2 (E), and 3 (F). Abundance changes relative to time point 1 are represented as mean (three biological replicates) ± standard deviation.
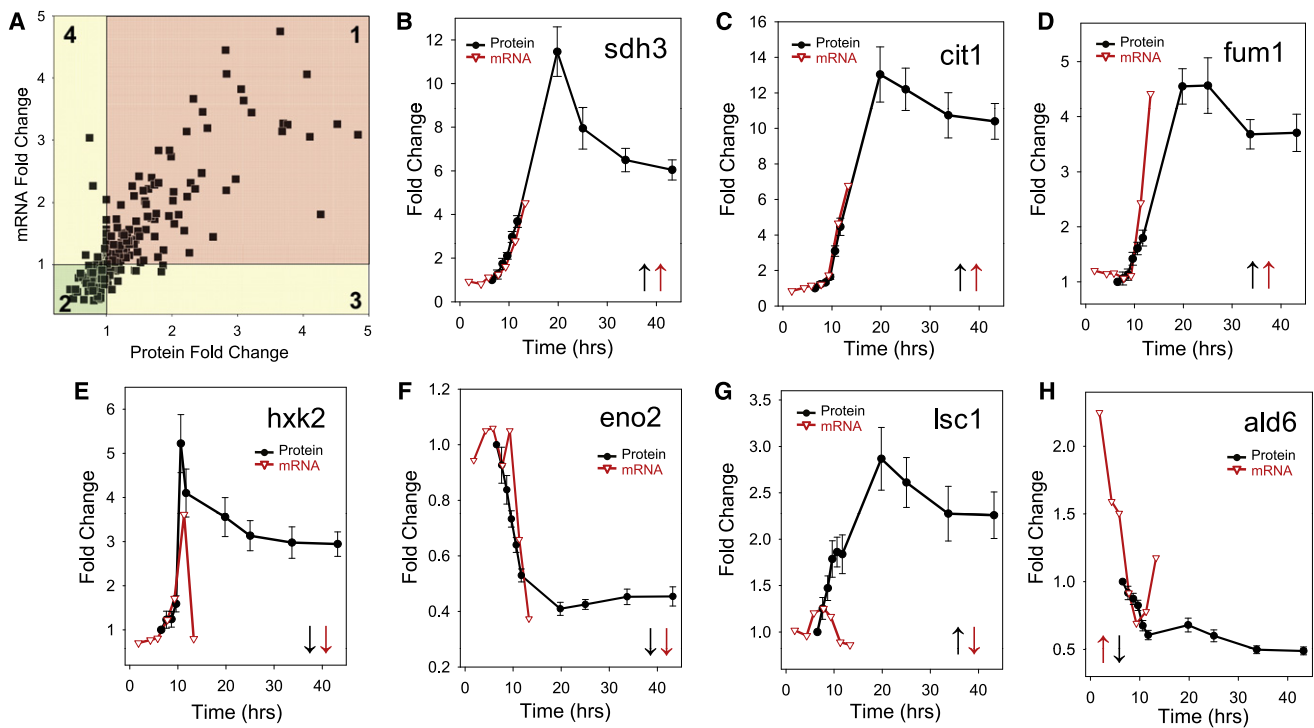
Figure 5. Comparison between Targeted Proteomics and Gene Expression Data

(A) Correlation between a protein and the corresponding transcript abundance fold change. Each point represents a given protein at a given time point. Four regions are highlighted: (1) protein and transcript abundance are both increasing, (2) both decreasing, (3) protein abundance increases while transcript abundance decreases, and (4) protein abundance decreases and transcript abundance increases.

(B–H) Overlay of a protein and the corresponding transcript abundance profiles. Representative examples are selected out of the four regions highlighted in (A). Protein abundance changes are reported as mean (three biological replicates) ± standard deviation. Transcript abundance changes are from DeRisi et al. (1997) after the realignment described in the Experimental Procedures.

predominantly the same direction of regulation is observed for a protein and its corresponding transcript. Representative examples for each pattern are shown in Figures 5B–5H, as overlaid time course profiles for a protein and the corresponding transcript. The availability of full protein and transcript time course data also allowed us to compare the magnitude and time dependency of the two data sets. In several cases we observed a striking synchronism and closely similar abundance fold changes (e.g., sdh3 and cit1 from group 1 or eno2 from group 2). In other cases, we observed a delayed response at the protein level (e.g., fum1, group 1). Further, in several cases at the decaying tail of an induction curve the transcript and protein profiles diverged, the protein levels persisting while the transcripts decayed (e.g., hxk2, group 2). Finally, for some proteins the direction of the abundance change was fully unanticipated by the gene expression data (e.g., lsc1, group 3; ald6, group 4). The time course proteomic data set and comparisons of the transcripts and protein profiles for each gene are available in the Supplemental Data (Figure S4 and Table S3).

DISCUSSION

A common requirement in molecular and cellular biology research is the ability to detect and quantify target proteins in biological samples, a need that became even more apparent with the

rise of systems biology. For the generation of mathematical models of protein networks (e.g., metabolic or signaling networks), in the context of systems biology research, it is crucial to measure all the elements that constitute the network under a set of different perturbing conditions. Frequently, such sets of proteins cover a wide range of physicochemical properties and cellular abundances that complicate their detection and quantification. Comprehensive proteomic measurements to face such challenge still suffer substantial limitations. This is optimally illustrated with the relatively simple eukaryotic organism *S. cerevisiae*, the species with the best characterized proteome to date. In spite of the considerable efforts worldwide, applying a range of experimental approaches, about 20% of the predicted yeast proteome has never been detected and, more generally, to date no proteome has been fully mapped yet. A main reason for this is the difficulty in detecting low-abundance proteins. However low-copy number proteins (<1000 copies/cell) are extremely attractive targets in systems biology research, since they often play a crucial role, e.g., as signal transducers, isoenzymes, or regulators of cellular processes. In the literature there are anecdotal reports claiming the detection of low-abundance proteins. However, these results were generally achieved in targeted studies in which a specific protein was studied, e.g., after affinity enrichment (Ghaemmaghami et al., 2003) or by large-scale proteomic studies whereby with intensive efforts the proteome

was extensively fractionated via multiple separation/enrichment steps prior to shotgun MS, resulting in identification of thousands of proteins (Chen et al., 2006; de Godoy et al., 2006, 2008). Although powerful, the latter studies require weeks of data acquisition and instrumental analysis per each single sample and are thus not practical when multiple samples and replicates have to be consistently analyzed, as is the case in dosage series or time course experiments required for systems biology.

Here we demonstrate that SRM-based proteomics has the power to detect and quantify yeast proteins expressed in the whole range of cellular abundance, down to less than 50 protein molecules/cell. Proteins could be detected in total yeast cell digests, without the need for sample fractionation or enrichment, making the use of the technique fast and practical. The technique is also highly multiplexed, supporting the detection and quantification of more than 100 different proteins, deliberately chosen and spanning all levels of abundance, in a single analysis. This allows to comprehensively monitor entire protein networks in a 1 hr MS run and thus to analyze in a reasonable time the effects on the system under study of different perturbing conditions and replicates. This satisfies in an ideal way the growing demand of systems biology for consistent, complete, and quantitative data sets from cells in differentially perturbed states. We illustrate the performance of targeted proteomics and the utility of the data by analyzing the dynamics of the proteins in the central carbon metabolism of *S. cerevisiae* over a complete growth time course, including a series of growth phases and a metabolic shift. This is, to date, the most complete quantitative data set describing the responses of each protein in the network to the series of events occurring during *S. cerevisiae* growth, at high temporal resolution. The whole SRM analysis required <2 days, and 30 samples were analyzed at the speed of 1 sample/hour, resulting in total 1350 protein abundance measurements. Previous attempts to capture by proteomics the events occurring upon glucose consumption during *S. cerevisiae* growth resulted in low coverage of the system under study (Futcher et al., 1999; Haurie et al., 2004) (13 and 15 out of the 45 proteins composing the system detected, respectively, with a clear bias toward the most abundant components). It is likely that the application of advanced shotgun proteomic methods involving extensive sample fractionation (de Godoy et al., 2008) would increase the coverage achieved by these studies, albeit at a significant cost in time, material, and labor.

Due to the lack of comprehensive, quantitative proteomic data sets, thus far the closest description of enzyme abundance changes upon glucose exhaustion in *S. cerevisiae* was derived from microarray studies (Brauer et al., 2005; DeRisi et al., 1997; Gasch et al., 2000; Radonjic et al., 2005). The strong induction observed in our study of all TCA and glyoxylate cycle enzymes and of fba1 and adh2 agrees with what previously extrapolated from transcriptomics data sets (although with different timing and regulation extent) and biochemical analyses. Thus, our data confirm the current view of a metabolic remodelling that redirects carbon fluxes from fermentative to respiratory pathways upon glucose exhaustion and thus release from glucose repression (Brauer et al., 2005; DeRisi et al., 1997; Polakis and Bartley, 1965). Specifically, this entails (1) the activation of the anaplerotic glyoxylate cycle to regenerate TCA intermediates,

(2) the reversion of glycolysis with consequent induction of key enzymes such as fbp1 that switch irreversible glycolytic steps, and (3) the activation of respiratory enzyme isoforms (e.g., adh2) (Brauer et al., 2005; DeRisi et al., 1997; Gasch and Werner-Washburne, 2002). Most of the protein expression differences persist through the postdiauxic phase until entrance to the stationary phase (this study; Radonjic et al., 2005). In addition, based on transcriptomic analyses it has been assumed that glycolytic enzymes and enzymes that control flow of metabolites to ethanol during fermentation (pdc1–6) undergo a decrease in abundance upon glucose exhaustion (Brauer et al., 2005; DeRisi et al., 1997; Gasch et al., 2000). This is in agreement with the reported lower glycolytic and pdc activity during respiratory growth (Entian and Zimmermann, 1980). Our data show that this extrapolation from transcriptomic data is not correct. Instead the abundance of glycolytic and pdc enzymes is not significantly changing throughout the whole growth profile, even though the corresponding transcripts decrease (see pdc1–6, fba1, pyk1, gpm1, gpm3, pgk1, pgi1, adh1, and pfk1, Figure S3). This suggests that potential posttrascriptional regulation of glycolysis and pdc activity occurs upon the diauxic shift in *S. cerevisiae*, in analogy to what was recently proposed for the metabolic adaptation of yeast to benzoic acid treatment and oxygen deprivation (Daran-Lapujade et al., 2007). Therefore our data set confirms previous knowledge but also carries a significant amount of new information, in terms of timing and regulation extent, for the protein network upon the metabolic shift that was not apparent from transcriptomic analyses alone, thus highlighting points of potential posttranscriptional regulation. This shows that accurate proteomic data sets such as the one generated in this study are required to provide a detailed picture of how protein networks adapt to changing conditions. The data set in particular provides an ideal framework for the improvement of mathematical models of metabolic reprogramming in *S. cerevisiae*. This overall confirms that the SRM approach provides a simple, economical, and fast way to explore the dynamics of cellular pathways, which will find broad applications in systems biology, but also in medical and pharmaceutical research (e.g., drug screening).

The results of the study also show that SRM detects proteins that have not been detectable before either by MS or quantitative western blotting, indicating that the number of proteins expressed in *S. cerevisiae* cells in log-phase growth is higher than previously reported (Ghaemmaghami et al., 2003). The data also suggest that it will now be possible to map out previously unknown segments of the yeast proteome, an advance that will also have significant implications for genome annotation.

The SRM technology showed a high success rate (~90%) in detecting proteins expressed in yeast cells. Examples of failed detection include highly modified proteins, cell wall or membrane proteins, or low-abundance proteins that lack PTPs with good MS properties (see Table S1). Variations of the technology applied here, e.g., the use of proteases different from trypsin, testing a higher number of PTPs in the case of highly modified proteins, or adapting the protein extraction procedure to detect membrane/cell wall proteins, will further increase the success in detecting previously undetected proteins.

The addition of a single step of peptide fractionation, performed by the well-established and fast technique of OGE,

further increased the sensitivity by on average one order of magnitude, thereby allowing the detection of proteins expressed at single-digit copies/cell concentration. The additional sensitivity provided by OGE might be exploited to detect difficult, low-abundance proteins that do not contain PTPs with good MS response or to follow the downregulation of proteins of low abundance. Targeting PTPs with pIs in the range 3–4.5, which showed the strongest signal gain in OGE fractions, can significantly increase the sensitivity of the SRM assay by up to 80 times (compared to the unfractionated samples).

When developing the SRM assays used in this work, a bottleneck step, in particular for low-abundance proteins, was the validation of the SRM transitions that constitute the definitive mass spectrometric assay in the type of mass spectrometer used for the measurements. This is typically achieved by acquiring a full fragment ion spectrum of the targeted peptides. For low intensity peptides, high quality fragment ion spectra are difficult to generate from full yeast digests due to the interference of the high level background. In such cases, validation required acquisition of the fragment ion spectra for the peptide in lower complexity sample (e.g., using OGE fractions). To facilitate the process we used unpurified synthetic peptides to develop and validate SRM assays for proteins that proved undetectable by other techniques. The use of such artificial proteomes strongly increased the confidence of the assay validation and increased the throughput in generating SRM assays. It is also particularly advantageous for targeting previously undetected proteins and therefore represents a significant advance in achieving complete proteome coverage by MS.

The final coordinates of SRM assays become universally useful and exportable. To this purpose, we developed a centralized web-based resource (Picotti et al., 2008) to store and allow the fast diffusion and usage of the SRM assays across different laboratories. The resource currently contains SRM assays for >1500 yeast proteins, including complete cellular pathways, such as the one shown in Figure 3.

In conclusion, this study demonstrates the potential of SRM-based proteomics to map out the whole observable yeast proteome by using assays to detect and quantify virtually any protein expressed at a concentration above single-digit copies/cell. It shows that quantitative assays for complete protein networks of interest can be developed and deployed to monitoring the dynamics of any network under study, across a high number of samples and replicates, at unprecedented speed, and with high quantitative accuracy. The described development of highly specific assays is generally applicable to any protein and proteomics project. These advances open a new avenue in the quantitative and qualitative analysis of proteins in the context of systems biology research and make the fast quantitative analysis of any protein in a proteome a concrete possibility.

EXPERIMENTAL PROCEDURES

Sample Preparation
Yeast cells were grown in two biological replicates to log phase at conditions closely matching those of Ghaemmaghami et al. (2003). Before lysis, aliquots of the cell suspension were subjected to cell counting in a Neubauer chamber and averaged results were expressed as cells/ml. Pelleted cells were disrupted by glass bead beating and proteins were precipitated by cold acetone,

reduced with 12 mM dithiotreitol, alkylated with 40 mM iodoacetamide, and digested with sequencing grade trypsin (Promega). Peptide samples were cleaned by Sep-Pak tC18 cartridges (Waters). The peptide mixtures were either directly destined to MS analysis or first separated by OGE using a pH 3–10 IPG strip (Amersham Biosciences) and a 3100 OFFGEL Fractionator (Agilent Technologies) with collection in 24 wells. Peptides collected in each well were cleaned as previously described and all peptide samples were evaporated to dryness and resolubilized in 0.1% formic acid for MS analysis.

In the time course experiments, yeast cells were grown in yeast extract peptone dextrose (20 g/L glucose) medium in triplicate. Cells sampled at each time point (from inoculation: 6.5, 7.6, 8.7, 9.6, 19.6, 11.7, 19.8, 25.0, 33.7, and 43.2 hr) were subjected to protein extraction and digestion. The optical density at 600 nm of the yeast cultures was measured regularly. Aliquots of the culture broth were analyzed with an HPLC system (Agilent HP1100) equipped with a refractive index detector and a UV/Vis detector (DAD) to determine the extracellular concentration of glucose and ethanol, using calibration curves constructed with external standards.

Design of SRM Assays
A set of *S. cerevisiae* proteins was selected containing proteins evenly distributed across the full range of cellular concentrations (Ghaemmaghami et al., 2003). Proteins that could not be detected by previous proteomic (Deutsch et al., 2008) or affinity-based (Ghaemmaghami et al., 2003) techniques were added to the list. For the network analysis a set of 45 proteins composing the core of carbon metabolism in *S. cerevisiae* was assembled. For each protein three to five PTPs were selected based on previous evidence (http://www.peptideatlas.org) (Deutsch et al., 2008) or by bioinformatic prediction using *PeptideSieve* (Mallick et al., 2007). For each peptide three to eight transitions for each of the two main charge states were calculated, corresponding to y series fragment ions. The transitions were used to detect the peptides in whole yeast protein digests or in OGE peptide fractions by SRM and to trigger acquisition of an MS/MS spectrum for each peptide. For proteins not observed in *PeptideAtlas* the five predicted PTPs were synthesized in an unpurified format, via the SPOT synthesis (JPT Peptide Technology), and used as a reference to develop the corresponding SRM assays.

MS Analysis
MS analyses were performed on a hybrid triple quadrupole/ion trap mass spectrometer (4000QTrap; ABI/MDS-Sciex). Chromatographic separations of peptides were performed on a Tempo nano LC system (Applied Biosystems) coupled to a 16 cm fused silica emitter, 75 μm diameter, packed with a Magic C18 AQ 5 μm resin (Michrom BioResources). Peptides (up to 3.5 μg of total protein digest) were separated with a linear gradient from 5% to 30% acetonitrile in 30 or 60 min, at a flow rate of 300 nl/min. In the SRM assays validation phase the mass spectrometer was operated in MRM mode, triggering acquisition of a full MS/MS spectrum upon detection of an SRM trace. Each SRM assay was validated by acquiring a full MS/MS spectrum for the peptide. For detailed information on the MS operating conditions see the Supplemental Experimental Procedures. Upon validation, the SRM assays were used to detect and/or quantify the proteins in total cell lysates and in each of the 24 OGE fractions, using scheduled SRM mode (retention time window, 180 s; target scan time, 3.5 s). Blank runs were performed regularly, in which the same set of transitions was monitored as in the following (sample) run. Blank runs were performed until no signal was detected for all transition traces, in particular prior to any measurement of low-abundance proteins. Where synthetic peptides were available, validation of peptide identities in yeast samples was based on the analogy of chromatographic and fragmentation properties to those of the standard. For low-abundance proteins the relative intensities of SRM traces were confirmed to match those of the corresponding fragment ions in the MS/MS spectrum of the peptide.

Database Search and Extraction of Optimal SRM Transitions
MS/MS spectra were assigned to peptide sequences by a target-decoy sequence database searching strategy using the tool Sequest. The search results were validated and assigned probabilities using the PeptideProphet program (Deutsch et al., 2008) with decoy-assisted semiparametric model and filtered as in Picotti et al. (2008). For each peptide, the three fragment

ions resulting in the highest signals were extracted from the triple quadrupole MS2 spectra (Picotti et al., 2008). The selected transitions were reanalyzed in scheduled SRM mode and the two peptides resulting in the maximal intensities were selected as final SRM assay for each protein. To accept validation of a set of SRM traces we checked that the retention time at which the MS2 spectrum was acquired matched that of the SRM peaks for the target peptide and we confirmed "coelution" of all SRM traces for the peptide. The SRM assay data set was uploaded to the MRMAtlas (http://www.mrmatlas.org) (Picotti et al., 2008) and is available in Tables S5 and S6.

Quantitative Analyses

For absolute quantification, isotopically labeled synthetic versions of the selected PTPs (see the Supplemental Experimental Procedures) were purchased from Thermo Fisher Scientific. The synthetic peptides were used for collision energy and declustering potential optimization. A known amount of heavy peptides was added prior to trypsinization to the protein mixtures. For relative quantification in the time course analyses each protein sample was mixed prior to trypsinization to an equal amount of yeast proteins extracted from ^{15}N-completely labeled yeast cells, used as an internal reference (see the Supplemental Experimental Procedures). The SRM assays were used to measure the peptides in the heavy and light versions using scheduled SRM.

Peak height for the transitions associated to the heavy and light peptides were quantified using the software MultiQuant v. 1.1 Beta (Applied Biosystems). Each transition for a given peptide was treated as an independent abundance measurement. Absolute quantification was obtained from the ratio between the light and heavy SRM peak height, multiplied by the known amount of the standard. Results were related to the number of cells processed and expressed in protein copies/cell as mean out of the different transitions, peptides, and the two biological replicates, ± the standard deviation. The potential contamination of the heavy peptide preparations with the corresponding unlabelled peptides was tested by injecting the heavy peptides alone and monitoring the transitions for both the heavy and light peptide forms. At the concentration used for quantitative measurements no signal was detectable in the "light" transitions.

For relative quantification of each protein across the growth time course the ratio between the light and heavy SRM peaks height was calculated and normalized to that obtained at the growth time point 1 (6.5. hr). Results were expressed as mean out of the different transitions/peptide, peptides/protein, and the three replicate cultures, ± the standard deviation and plotted using SigmaPlot (Systat Software). Outlier transitions (e.g., shouldered transition traces or noisy transitions with S/N < 3) were not considered in the calculations.

Time Course Data Analysis

Protein time course profiles were compared to transcript data (DeRisi et al., 1997). The data sets were realigned using the transition midpoints and the glucose consumption curves and overlaid (Figures 5B–5H). A comparison of the protein and transcript fold changes was performed in the growth time frame covered by both data sets, normalizing transcript fold changes to the first common sampling point. When sampling was performed at different time intervals, transcript fold changes at matching points was linearly extrapolated from the two closest measured time points.

The log$_{10}$ transformed profiles of the mean protein fold changes were subjected to K-means clustering (Macqueen, 1967) (four initial clusters). A Student's paired t test was performed to determine statistically significant changes in protein abundances upon the metabolic shift. The threshold for statistical significance was $p < 0.05$ and an abundance change >2-fold (Table S4).

SUPPLEMENTAL DATA

Supplemental Data include Supplemental Discussion, Supplemental Experimental Procedures, four figures, and six tables and can be found with this article online at http://www.cell.com/supplemental/S0092-8674(09)00715-6.

REFERENCES

Aebersold, R., and Mann, M. (2003). Mass spectrometry-based proteomics. Nature *422*, 198–207.

Anderson, L., and Hunter, C.L. (2006). Quantitative mass spectrometric multiple reaction monitoring assays for major plasma proteins. Mol. Cell. Proteomics *5*, 573–588.

Brauer, M.J., Saldanha, A.J., Dolinski, K., and Botstein, D. (2005). Homeostatic adjustment and metabolic remodeling in glucose-limited yeast cultures. Mol. Biol. Cell *16*, 2503–2517.

Brunner, E., Ahrens, C.H., Mohanty, S., Baetschmann, H., Loevenich, S., Potthast, F., Deutsch, E.W., Panse, C., de Lichtenberg, U., Rinner, O., et al. (2007). A high-quality catalog of the *Drosophila melanogaster* proteome. Nat. Biotechnol. *25*, 576–583.

Chen, E.I., Hewel, J., Felding-Habermann, B., and Yates, J.R., 3rd. (2006). Large scale protein profiling by combination of protein fractionation and multidimensional protein identification technology (MudPIT). Mol. Cell. Proteomics *5*, 53–56.

Daran-Lapujade, P., Rossell, S., van Gulik, W.M., Luttik, M.A., de Groot, M.J., Slijper, M., Heck, A.J., Daran, J.M., de Winde, J.H., Westerhoff, H.V., et al. (2007). The fluxes through glycolytic enzymes in *Saccharomyces cerevisiae* are predominantly regulated at posttranscriptional levels. Proc. Natl. Acad. Sci. USA *104*, 15753–15758.

de Godoy, L.M., Olsen, J.V., de Souza, G.A., Li, G., Mortensen, P., and Mann, M. (2006). Status of complete proteome analysis by mass spectrometry: SILAC labeled yeast as a model system. Genome Biol. *7*, R50.

de Godoy, L.M., Olsen, J.V., Cox, J., Nielsen, M.L., Hubner, N.C., Frohlich, F., Walther, T.C., and Mann, M. (2008). Comprehensive mass-spectrometry-based proteome quantification of haploid versus diploid yeast. Nature *455*, 1251–1254.

DeRisi, J.L., Iyer, V.R., and Brown, P.O. (1997). Exploring the metabolic and genetic control of gene expression on a genomic scale. Science *278*, 680–686.

Desiderio, D.M., and Kai, M. (1983). Preparation of stable isotope-incorporated peptide internal standards for field desorption mass spectrometry quantification of peptides in biologic tissue. Biomed. Mass Spectrom. *10*, 471–479.

Deutsch, E.W., Lam, H., and Aebersold, R. (2008). PeptideAtlas: a resource for target selection for emerging targeted proteomics workflows. EMBO Rep. *9*, 429–434.

Domon, B., and Broder, S. (2004). Implications of new proteomics strategies for biology and medicine. J. Proteome Res. *3*, 253–260.

Entian, K.D., and Zimmermann, F.K. (1980). Glycolytic enzymes and intermediates in carbon catabolite repression mutants of *Saccharomyces cerevisiae*. Mol. Gen. Genet. *177*, 345–350.

Futcher, B., Latter, G.I., Monardo, P., McLaughlin, C.S., and Garrels, J.I. (1999). A sampling of the yeast proteome. Mol. Cell. Biol. *19*, 7357–7368.

Gasch, A.P., and Werner-Washburne, M. (2002). The genomics of yeast responses to environmental stress and starvation. Funct. Integr. Genomics *2*, 181–192.

Gasch, A.P., Spellman, P.T., Kao, C.M., Carmel-Harel, O., Eisen, M.B., Storz, G., Botstein, D., and Brown, P.O. (2000). Genomic expression programs in the response of yeast cells to environmental changes. Mol. Biol. Cell *11*, 4241–4257.

Gerber, S.A., Rush, J., Stemman, O., Kirschner, M.W., and Gygi, S.P. (2003). Absolute quantification of proteins and phosphoproteins from cell lysates by tandem MS. Proc. Natl. Acad. Sci. USA *100*, 6940–6945.

Ghaemmaghami, S., Huh, W.K., Bower, K., Howson, R.W., Belle, A., Dephoure, N., O'Shea, E.K., and Weissman, J.S. (2003). Global analysis of protein expression in yeast. Nature *425*, 737–741.

Haurie, V., Sagliocco, F., and Boucherie, H. (2004). Dissecting regulatory networks by means of two-dimensional gel electrophoresis: application to the study of the diauxic shift in the yeast *Saccharomyces cerevisiae*. Proteomics *4*, 364–373.

Hilpert, K., Winkler, D.F., and Hancock, R.E. (2007). Peptide arrays on cellulose support: SPOT synthesis, a time and cost efficient method for synthesis of large numbers of peptides in a parallel and addressable fashion. Nat. Protoc. *2*, 1333–1349.

Kuster, B., Schirle, M., Mallick, P., and Aebersold, R. (2005). Scoring proteomes with proteotypic peptide probes. Nat. Rev. Mol. Cell Biol. *6*, 577–583.

Lange, V., Malmstrom, J.A., Didion, J., King, N.L., Johansson, B.P., Schafer, J., Rameseder, J., Wong, C.H., Deutsch, E.W., Brusniak, M.Y., et al. (2008). Targeted quantitative analysis of *Streptococcus pyogenes* virulence factors by multiple reaction monitoring. Mol. Cell. Proteomics *7*, 1489–1500.

Macqueen, J. (1967). Some methods for classification and analysis of multivariate observations. In Proceedings of the 5th Berkeley Symposium on Mathematical Statistics and Probability (Berkeley, CA: University of California Press), pp. 281–297.

Mallick, P., Schirle, M., Chen, S.S., Flory, M.R., Lee, H., Martin, D., Ranish, J., Raught, B., Schmitt, R., Werner, T., et al. (2007). Computational prediction of proteotypic peptides for quantitative proteomics. Nat. Biotechnol. *25*, 125–131.

Malmstrom, J., Lee, H., Nesvizhskii, A.I., Shteynberg, D., Mohanty, S., Brunner, E., Ye, M., Weber, G., Eckerskorn, C., and Aebersold, R. (2006). Optimized peptide separation and identification for mass spectrometry based proteomics via free-flow electrophoresis. J. Proteome Res. *5*, 2241–2249.

Pawlak, M., Schick, E., Bopp, M.A., Schneider, M.J., Oroszlan, P., and Ehrat, M. (2002). Zeptosens' protein microarrays: a novel high performance microarray platform for low abundance protein analysis. Proteomics *2*, 383–393.

Picotti, P., Aebersold, R., and Domon, B. (2007). The implications of proteolytic background for shotgun proteomics. Mol. Cell. Proteomics *6*, 1589–1598.

Picotti, P., Lam, H., Campbell, D., Deutsch, E., Mirzaei, H., Ranish, J., Domon, B., and Aebersold, R. (2008). A database of mass spectrometric assays for the yeast proteome. Nat. Methods *5*, 913–914.

Polakis, E.S., and Bartley, W. (1965). Changes in the enzyme activities of *Saccharomyces cerevisiae* during aerobic growth on different carbon sources. Biochem. J. *97*, 284–297.

Radonjic, M., Andrau, J.C., Lijnzaad, P., Kemmeren, P., Kockelkorn, T.T., van Leenen, D., van Berkum, N.L., and Holstege, F.C. (2005). Genome-wide analyses reveal RNA polymerase II located upstream of genes poised for rapid response upon *S. cerevisiae* stationary phase exit. Mol. Cell *18*, 171–183.

Stahl-Zeng, J., Lange, V., Ossola, R., Eckhardt, K., Krek, W., Aebersold, R., and Domon, B. (2007). High sensitivity detection of plasma proteins by multiple reaction monitoring of N-glycosites. Mol. Cell. Proteomics *6*, 1809–1817.

Taussig, M.J., Stoevesandt, O., Borrebaeck, C.A., Bradbury, A.R., Cahill, D., Cambillau, C., de Daruvar, A., Dubel, S., Eichler, J., Frank, R., et al. (2007). ProteomeBinders: planning a European resource of affinity reagents for analysis of the human proteome. Nat. Methods *4*, 13–17.

Uhlen, M. (2008). Affinity as a tool in life science. Biotechniques *44*, 649–654.

Uhlen, M., and Hober, S. (2009). Generation and validation of affinity reagents on a proteome-wide level. J Mol. Recognit. *22*, 57–64.

Wenschuh, H., Volkmer-Engert, R., Schmidt, M., Schulz, M., Schneider-Mergener, J., and Reineke, U. (2000). Coherent membrane supports for parallel microsynthesis and screening of bioactive peptides. Biopolymers *55*, 188–206.

Wolf-Yadlin, A., Hautaniemi, S., Lauffenburger, D.A., and White, F.M. (2007). Multiple reaction monitoring for robust quantitative proteomic analysis of cellular signaling networks. Proc. Natl. Acad. Sci. USA *104*, 5860–5865.